32 p. 008

N64 23994 Code 23

code 1 CR56620

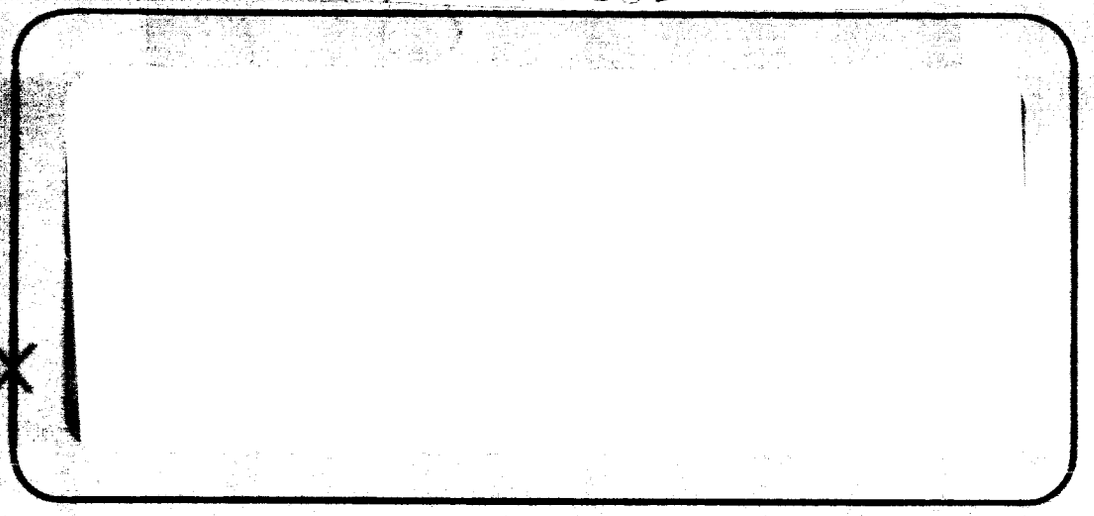

TRW SPACE TECHNOLOGY LABORATORIES

THOMPSON RAMO WOOLDRIDGE INC.

One Space Park · Redondo Beach, California

Also Appl SGP 2 July 64

OTS PRICE

XEROX $ 3.60 ph

MICROFILM $ _____

8888-6006-SU-000

30 November 1963

Final Report NASw-561

INVESTIGATION OF HIGH-SPEED IMPACT PHENOMENA (II)

Prepared for:

NASA Headquarters
Code (sc)
Washington 25, D.C.

Contract No. NASw-561

J. F. Friichtenicht

Prepared by
J. F. Friichtenicht

D. B. Langmuir

Approved by
D. B. Langmuir
Director

PHYSICAL ELECTRONICS LABORATORY
Physical Research Division

TRW Space Technology Laboratories
One Space Park
Redondo Beach, California

TABLE OF CONTENTS

		Page
	FIGURE CAPTIONS.	ii
I.	Introduction	1
II.	Experimental Techniques.	2
III.	Experimental Results	6
	A. Impact Ionization Effect.	6
	B. Impact Light Flash.	16
	C. Gaseous Target Impacts.	20
	D. Miscellaneous Tests and Experiments	26
IV.	Summary.	27
	REFERENCES	29

FIGURE CAPTIONS

Page

Figure 1. Schematic diagram of charged particle detector with conventional and "bootstrapped" cathode follower inputs. 5

Figure 2. Experimental arrangement for the measurement of impact ionization from thick target impacts 7

Figure 3. Tracing of an oscillograph obtained from the thick target measurements on impact ionization. 9

Figure 4. Charge collected normalized to r^3 plotted as a function of particle velocity for iron particle impacts on a thick tantalum target. 11

Figure 5. Q/r^3 vs. v for iron particle impacts on several target materials 12

Figure 6. Charge collected normalized to the number of atoms in the particle as a function of velocity for carbon and iron particle impacts on a tungsten target 14

Figure 7. Charge collected normalized to the number of atoms in the particle as a function of velocity for carbon and iron particle impacts on a lead target. 15

Figure 8. Light flash amplitude normalized to particle mass as a function of particle velocity for a glass target. 19

Figure 9. Curves illustrating the simulation of meteors. 25

INVESTIGATION OF HIGH SPEED IMPACT PHENOMENA

I. INTRODUCTION

This report summarizes the program of research conducted under NASA Contract No. NASw-561 for the period from 31 October 1962 to 30 November 1963. Under the terms of this contract, experimental investigations of several aspects of high-speed impact phenomena were conducted using the TRW Space Technology Laboratories' 2-million-volt electrostatic hypervelocity projector as a source of high-speed particles. In general, the experiments which have been conducted are related to the field of meteoritics in one form or another.

Two earlier contracts (NAS5-763 and NASw-269) enabled us to develop techniques and to specify problem areas where the electrostatic accelerator could be used to best advantage. During the period covered by this report, experiments which are directly applicable to specific problems of micrometeoroid simulation were conducted. An example of this type of experiment is the interaction of high-speed particles with gaseous targets. These experiments provide data which will be useful in assessing the properties of photographic meteors.

Another major area of interest is the continued investigation of properties of high-speed impact which are applicable to micrometeoroid detector systems. As in the past, this type of experiment has been more concerned with the basic properties of the impact process as opposed to the development of instruments or systems. However, sensor systems utilizing some of the effects investigated under the earlier contracts have been developed by NASA personnel and joint tests of them have been accomplished using the STL facilities.

The work accomplished in each of these areas will be summarized in the following sections. Reference should be made to the Quarterly Progress Reports and Technical Reports which have been submitted for more detailed information regarding some of the work which has been done.

II. EXPERIMENTAL TECHNIQUES

Many of the procedures followed in conducting this program of research were common to all of the experiments and have been described in some detail in other reports.[1,2] In most of the experiments the projectiles were iron spheres ranging in size from about 0.2 to 1.5 microns radius. The smaller particles achieved velocities in excess of 10 km/sec, while the velocities of the larger ones were 2 km/sec, or less. The average iron particle was about 1.5 microns in diameter and achieved a velocity of about 5 km/sec. Some experiments made use of carbon black (graphite) particles which, because of their reduced density, achieved somewhat higher velocities. The carbon particles averaged about 0.6 micron in diameter and achieved velocities in the 6 to 16 km/sec range.

The velocity and mass of the particles were measured by detectors of the type described in Refs. 1 and 2. The charge on the accelerated particle is determined by measuring the amplitude of the voltage signal induced on a cylindrical drift tube of known capacitance to ground as the particle passes along its axis. The duration of the signal is simply the time required by the particle to traverse the electrical length of the tube. The velocity of the particle is determined in this manner. The mass of the particle is computed from the conservation of energy equation: $m = 2qV/v^2$, where v is the velocity, q the charge, and V the total accelerating voltage.

The geometry of the charged particle detectors was varied to fit the requirements of specific experiments. A number of detector configurations were used, but the principle of operation was the same in all cases.

For most of the measurements, the detector signal was amplified and displayed on one beam of a Tektronix 551 dual-beam oscilloscope. In the cases where the information from the experiment in question was in the form of an electrical signal, the information was displayed on the other beam. Usually, both beams were triggered by the detector signal so that time-of-flight techniques could be employed to establish an exact correlation between the particles and the observed impact effects. Photographs of the oscilloscope traces provided permanent records of the events.

A new method of data reduction from the photographs has been developed recently which reduces data reduction time and increases the accuracy of the readings. A computer program was written for the IBM-7090 computer. Provision was made to adjust values for all of the parameters required for the solution of the conservation of energy equation. In practice, the length and height of the detector signal are read by means of a Tele-reader to three-figure accuracy and this information is automatically punched onto the computer cards. A third experimental quantity, for example, the impact light flash amplitude, may be punched on the cards in a similar manner. These cards, along with the program cards which specify the fixed parameters, are then fed to the computer. The print-out includes an identification number, the values of all of the input parameters, and the computed values of particle mass, radius, velocity, charge, momentum, and kinetic energy. This technique reduces data reduction time by an order of magnitude, and it will be used extensively in future experiments.

Another recent innovation has been the development of a much more sensitive charged particle detector preamplifier. This detector preamplifier is capable of detecting charges of 10^{-16} coulombs or less which means that much smaller particles can be detected. Since the smaller particles achieve higher velocities, the effective velocity range of particles from the Van de Graaff has been increased. Many iron particles with velocities in excess of 20 km/sec have been observed with this detector.

Since the charged particle is detected by the voltage induced on the capacitance of a detector element as the particle passes through it, smaller charges may be detected by decreasing the capacitance. The effective capacitance has been decreased by a "bootstrapping" technique.

Two forms of a cathode follower detector input stage are illustrated in Fig. 1. Figure 1-a is a conventional cathode follower, where C_D is the capacitance of the detector to ground. For a particle of charge q, the signal induced at the grid is $V_g = q/C_D$. If the gain of the cathode follower is G the output voltage is GV_g.

Figure 1-b is a bootstrapped cathode follower. The detector is surrounded by a cylindrical shield which is tied to the cathode of the tube. C_D is the capacitance between the detector and the shield while C_S is the capacitance of the shield to ground. As before, a particle passing through the detector induces a voltage across C_D given by $V = q/C_D$. The grid voltage V_g is the sum of the voltages on C_D and C_S, but the voltage on C_S is the output voltage GV_g. Thus the grid voltage is $V_g = q/C_D + GV_g$ or $V_g = q/(1 - G)C_D$ and the detector capacitance has been effectively reduced by the factor $(1 - G)$. A typical cathode follower has a gain of about 0.9 so the effective gain is about a factor of 10 greater.

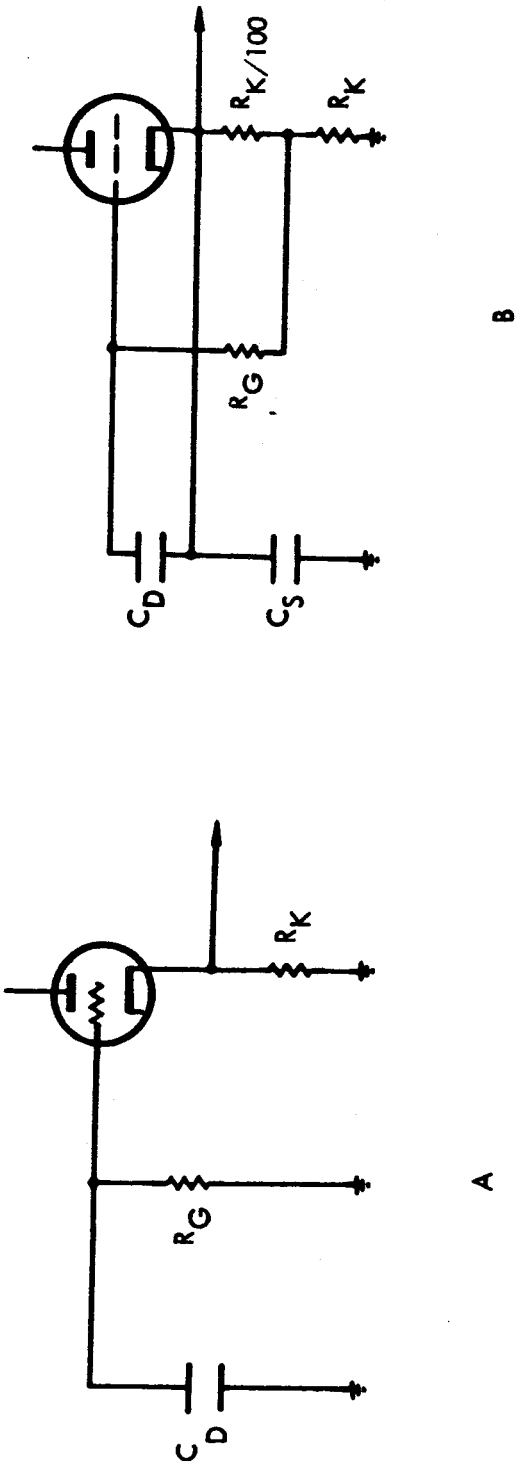

Figure 1. Schematic diagram of charged particle detectors with conventional and "bootstrapped" cathode follower inputs.

The operation of the accelerator has not been altered to any significant extent. The charged-particle injector is controlled and actuated from the Van de Graaff control console by the operator. The frequency of injection and the number of particles injected at any one time is at the discretion of the operator. For most of our work, we are concerned with the effects of single particle impact and, consequently, only a few particles (and frequently one or none) were injected at a time.

III. EXPERIMENTAL RESULTS

As mentioned above, the program of research has encompassed a variety of experiments. Each of these will be discussed in the following paragraphs.

A. Impact Ionization Effect

From our earlier work, we have concluded that some of the atoms near the impact site of a high-speed particle are ionized by the large energy release associated with the impact. The emitted charge (either positive or negative) can be collected by means of electrically biased collectors and the resulting signal may be used in various types of meteoroid detectors. The quantity of charge emitted depends upon particle velocity and mass, and upon characteristics of the materials in question.

The geometrical configuration of the detector and collector system used in examining charge emission from thick targets is illustrated in Fig. 2. Particles from the accelerator pass along the axis of a velocity-charge detector, pass through a grid structure, and impact upon the surface of the target sample at normal incidence. For all of the measurements discussed here, the target was biased 300 volts negative with respect to the grounded grid. With this bias, negative charge produced at the target surface is

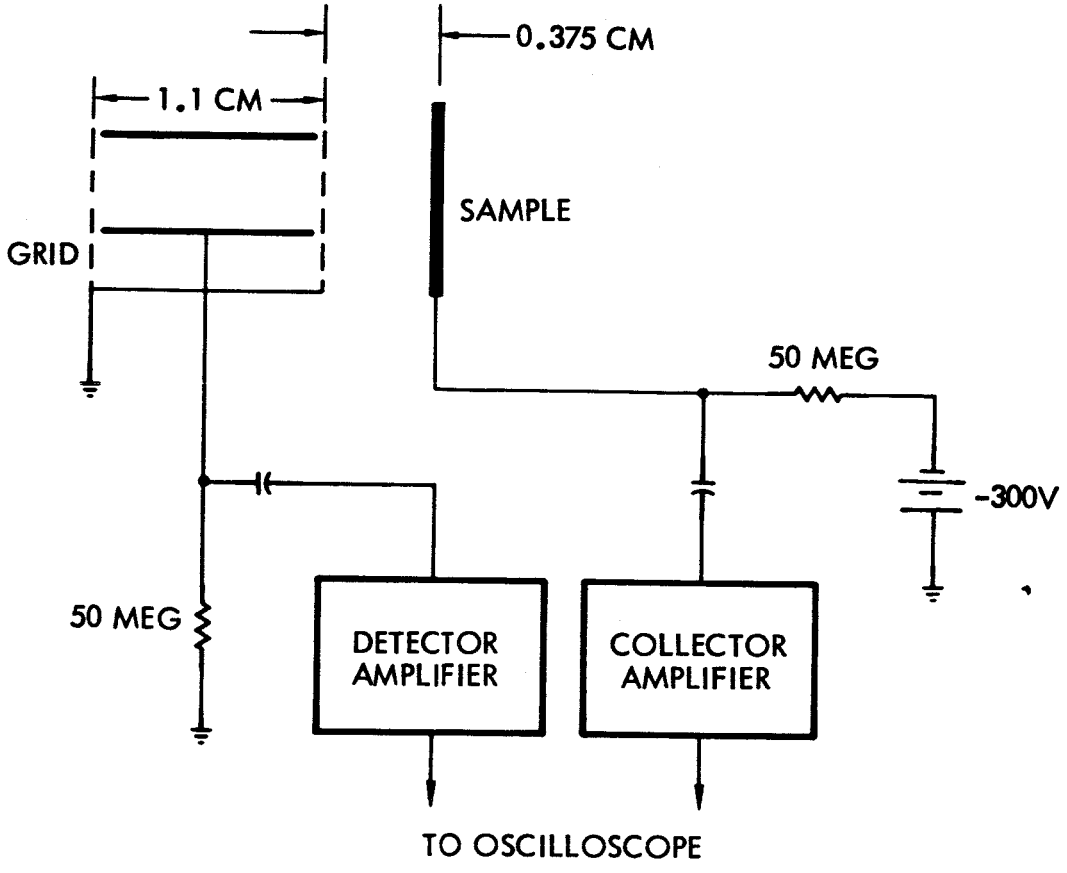

Figure 2. Experimental arrangement for the measurement of impact ionization from thick target impacts.

repelled from the collector while positive charge is retained. The quantity of charge retained by the target is determined from the relationship $Q_c = CV$, where C is the electrical capacitance of the collector and V is the amplitude of the induced voltage signal. The RC time constant of the collector system was made long compared to the signal duration so that the signal is proportional to charge as opposed to current flow. We have previously determined that the quantity of collected charge was nearly independent of the polarity and magnitude of the bias voltage for biases exceeding a few tens of volts. For this work, the choice of bias voltage and polarity was made arbitrarily and it is assumed that corresponding results would be obtained with different choices.

Figure 3 is a tracing of a typical photographic record of an event. In this case, a copper target sample was used. The particle detector signal is displayed on the lower trace while the collected charge signal appears on the upper trace. Since the impacting particle is charged, a voltage signal is induced on the collector independently of that produced by subsequent charge emission. This effect accounts for the structure on the upper trace. The particle charge produces the first step in the signal, while the charge emission effect accounts for the remainder. The total charge emitted is obtained by subtracting the particle charge from the total signal. In cases where the signal from the particle charge was small compared to the total, the particle charge was determined from the particle detector.

Since few theoretical guidelines were available to assist us in interpretation of the experiments, the data were analyzed on a more or less empirical basis. We assume that the quantity of charge emitted, Q_c, is proportional to the kinetic energy of the particle modified by a velocity dependent function which takes into account threshold effects and variations of cratering mechanisms with velocity. This is equivalent to

$$\frac{Q_c}{m} = K\, v^2\, f(v) \quad , \qquad (1)$$

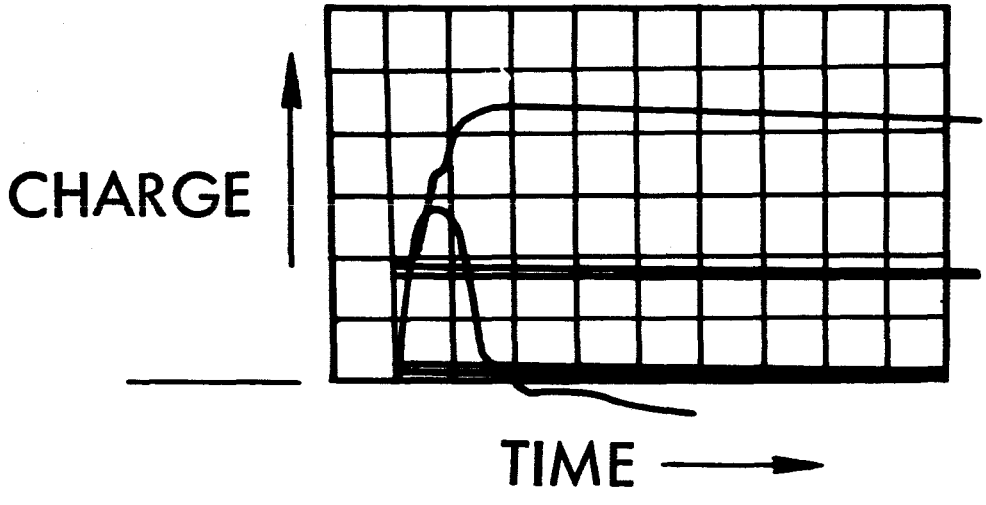

Figure 3. Tracing of an oscillograph obtained from the thick target measurements on impact ionization.

where m is the particle mass and K is a constant of proportionality.

To evaluate f(v), the quantity Q_c/r^3 (which is equivalent to Q_c/m, for a given particle material) was plotted as a function of velocity for all of the particle-target combinations used. A typical example is illustrated in Fig. 4, which shows the results for iron particles impinging on a tantalum target. These data exhibit little scatter and the points tend to lie on a straight line in the logarithmic presentation. The slope of the line is about three as was the case for all of the other target and particle combinations used. This implies that $f(v) \approx v$. Consequently, we can write

$$Q_c = Kmv^3 \quad . \tag{2}$$

The constant K appears to be a function of material properties of the target and particle. The dependence on target material is illustrated in Fig. 5, where smoothed curves are plotted for each of the targets used. These data were obtained with iron particles. It can be seen that the materials examined fall into two distinct categories. More charge is emitted from the Ta, W, and Pt targets than from targets of Cu, Be-Cu, In, and Pb. With the possible exception of lead, all of the targets exhibit nearly identical results.

It is almost a certainty that the quantity of charge emitted is a function of more than one characteristic of the target material. Because of the complexity of the problem, no attempt has been made to explain the material dependence. However, certain characteristics of the materials exhibit a similar grouping. For example, Ta, W, and Pt all have higher melting and vaporization temperatures than the others. Also, these same materials are classified as good thermionic emitters, while the others are not.

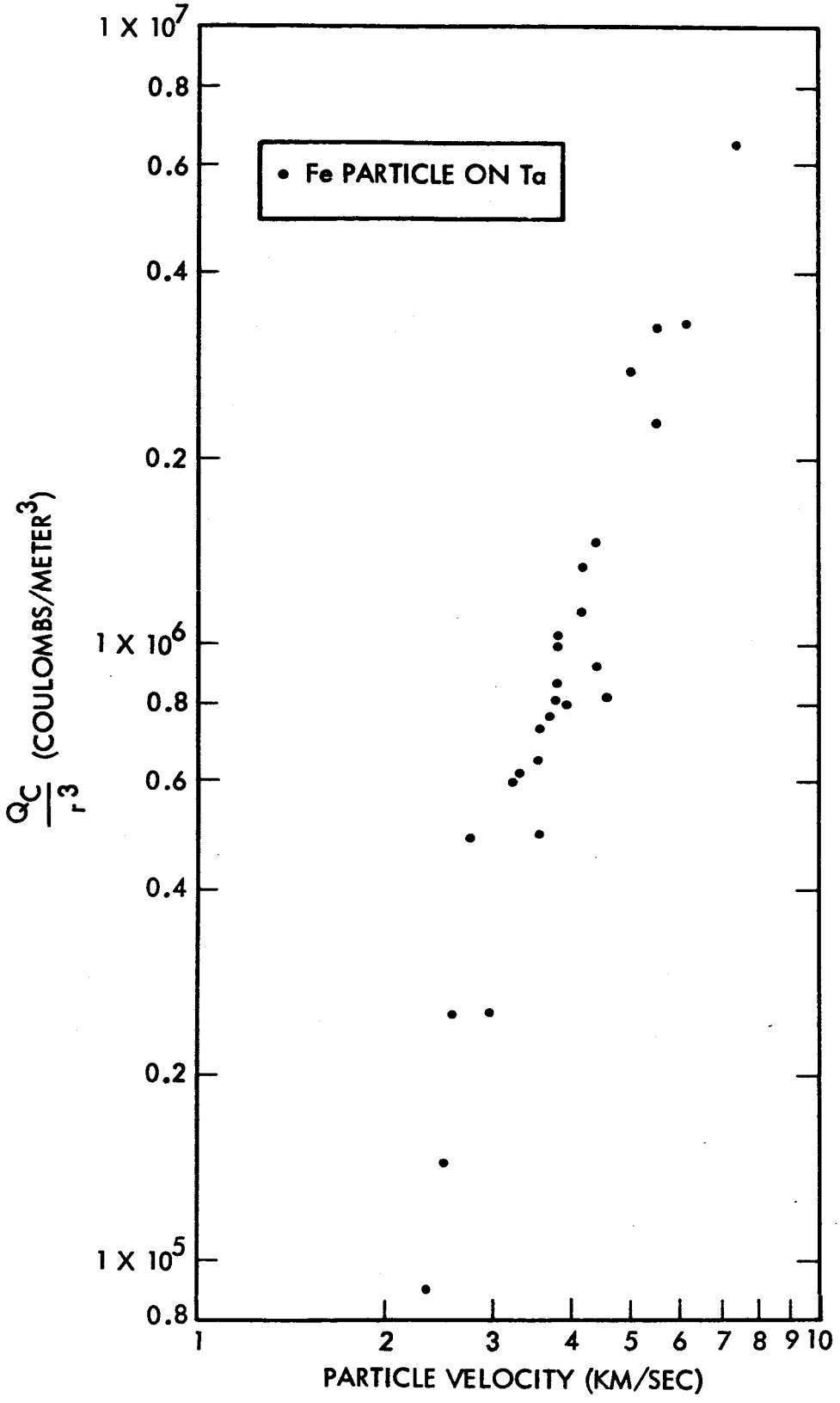

Figure 4. Charge collected normalized to r^3 plotted as a function of particle velocity for iron particle impacts on a thick tantalum target.

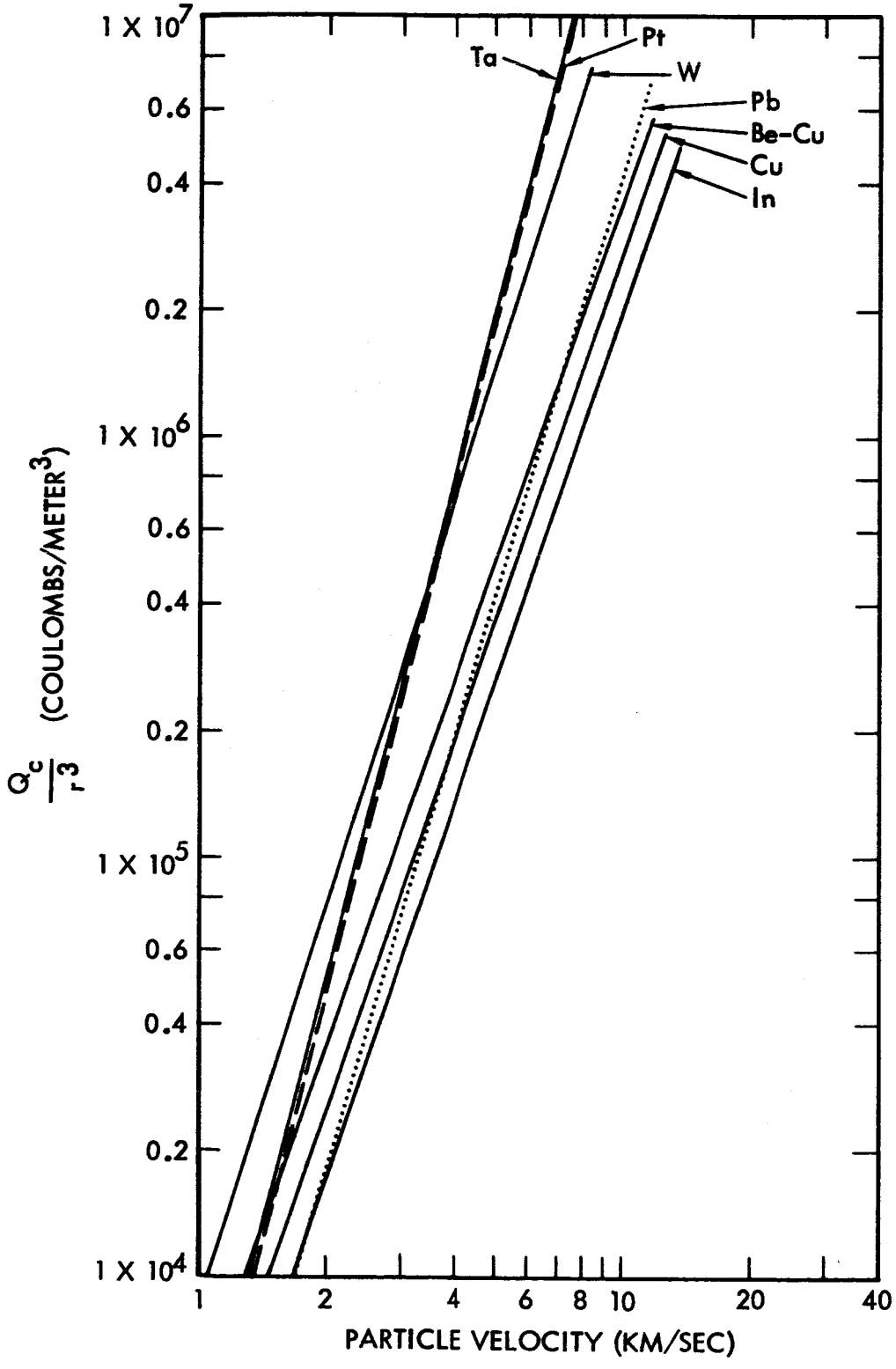

Figure 5. Q/r^3 vs. v for iron particle impacts on several target materials.

Perhaps the most significant property of all is that of resistance to hypervelocity penetration. The craters produced in Pb, In, Cu, and Be-Cu are generally larger than those in Ta, Pt, and W.

The dependence of K, in Eq. 2 above, on particle material was observed when iron particle data and carbon particle data were compared. When normalized to particle mass, the amount of charge produced by carbon particles was greater than that produced by iron particles at a given impact velocity for the same target. Initially, we assumed that the bulk of the emitted charge resulted from ionization of atoms of the target material. Application of several combinations of hypervelocity penetration theories and charge production mechanisms failed to rationalize the discrepancy. Failure to achieve correlation in this manner led to the development of the model discussed below.

Let us assume that most of the charge results from ionization of atoms of the impacting particle. The number of atoms ionized depends upon the number available, the energy required for ionization, and the energy available for ionization. The kinetic energy of the particle is dissipated in several ways and the relative amount available for ionization is impossible to predict on the basis of existing knowledge of hypervelocity impact. At this point, we arbitrarily chose to normalize the emitted charge to the number of atoms contained in the impacting particle. This quantity, Q_c/N, is plotted as a function of velocity for iron and carbon particle impacts on a tungsten target in Fig. 6, and for a lead target in Fig. 7. Since N is proportional to m, the same v^3 dependence is obtained. However, the agreement between the results of using iron and carbon particles is quite good in this case.

Normalization to the number of atoms is equivalent to the following expression:

$$Q_c = K_1 \left(\frac{N_o}{A} \right) mv^3 \quad , \tag{3}$$

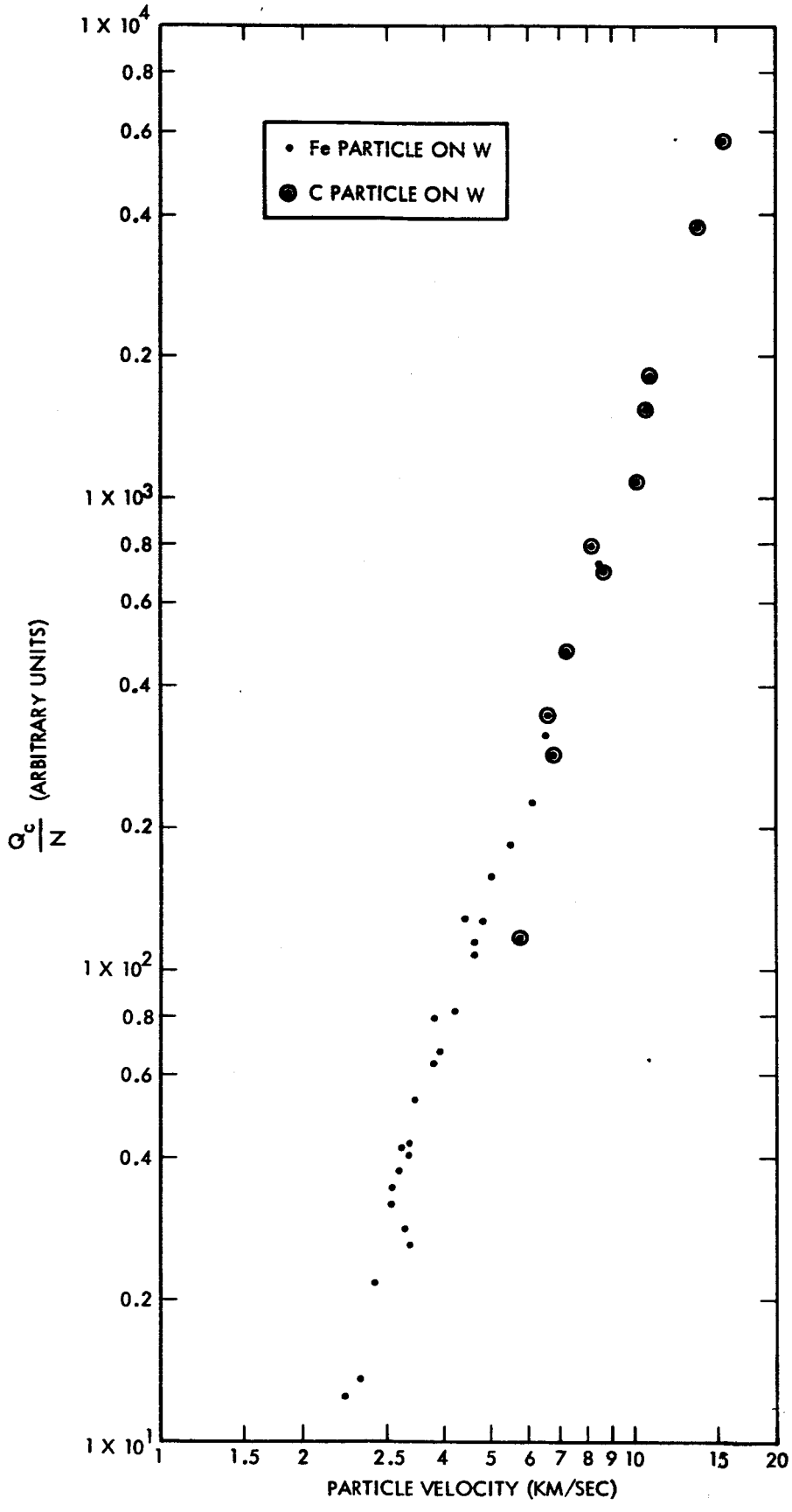

Figure 6. Charge collected normalized to the number of atoms in the particle as a function of velocity for carbon and iron particle impacts on a tungsten target.

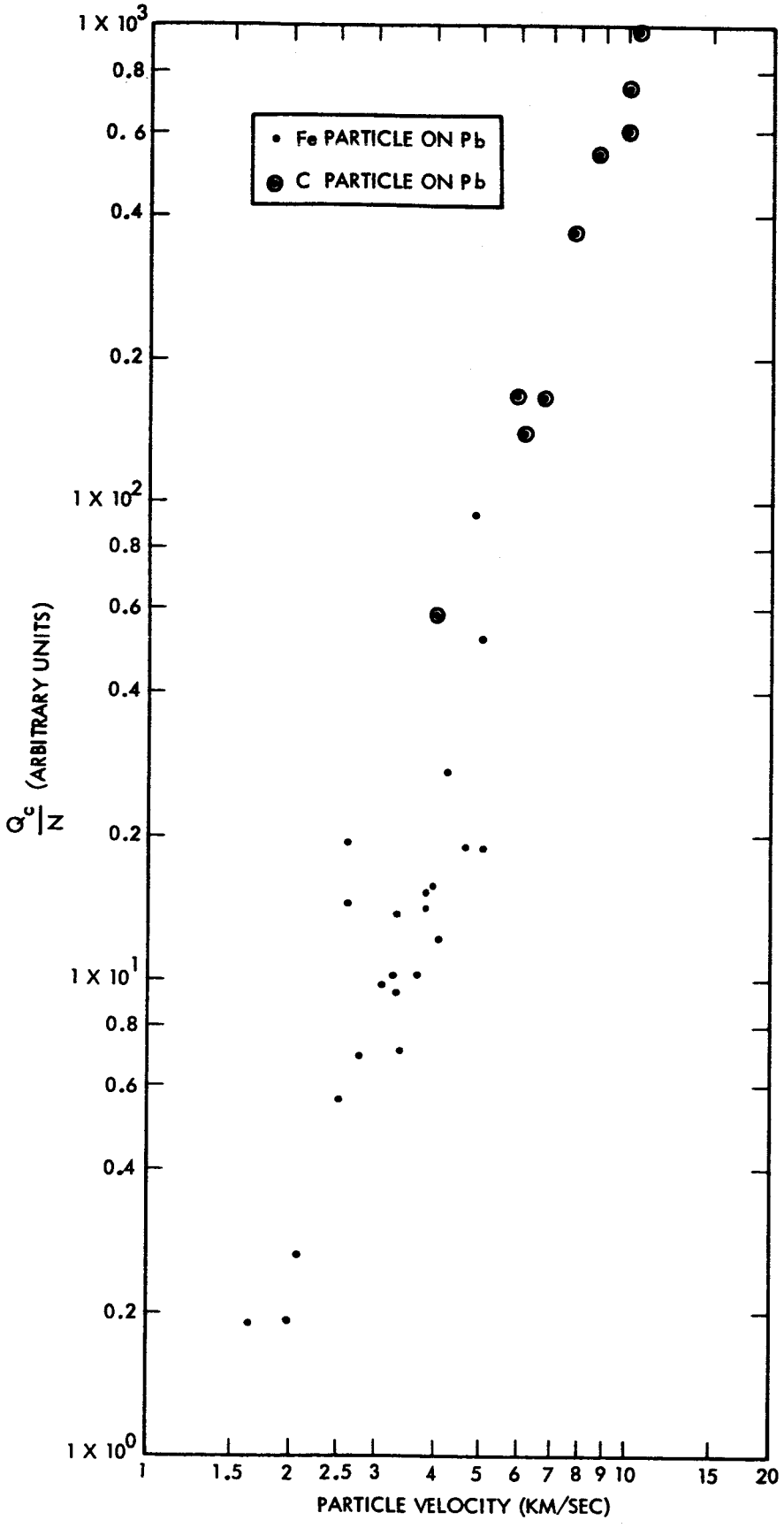

Figure 7. Charge collected normalized to the number of atoms in the particle as a function of velocity for carbon and iron particle impacts on a lead target.

where N_o is Avogadros number, A the molecular weight of the particle atoms, and K_1 a constant of proportionality. Equation (3) can be rewritten in the form

$$Q_c = K_2 E_p \frac{v}{A} \quad . \tag{4}$$

From this, we see that Q_c depends upon the kinetic energy of the particle and upon a quantity which can be interpreted as a factor which determines the fractional part of the energy which is available for ionization. The role of the target, in this interpretation, is simply that of resisting penetration by the particle. The higher the resistance; the larger the fraction of energy which goes into ionization. More detailed information concerning these measurements has been included in an earlier report.[3]

The problem resulting from empirical data analysis is that one has difficulty in attaching physical significance to the results. The choice of v/A as a multiplying factor is strictly empirical and we cannot justify it from a physical point of view. Despite these drawbacks, one must have a framework within which to work, and the approach used in the preceding section provides such a framework. Additional experiments and analysis should be undertaken to develop physical concepts to describe the charge emission phenomenon.

B. Impact Light Flash

Another feature of high-speed impact which has found application in micrometeoroid detector systems[4,5] is the so-called impact light flash. It has been observed that part of the kinetic energy of a high-speed particle is converted to radiant energy upon impact with a solid target. The existence of a light flash in a vacuum environment was verified under a prior contract (NAS5-763).

However, only qualitative results were obtained. The experiments described below are the first steps in a program to obtain more quantitative data.

For micrometeoroid detector systems, correlation of some property of the impact light flash with parameters of the impacting particle is desirable. A more subtle application of this effect is in the area of hypervelocity impact. Only recently have the effects of melting and vaporization been included in hypervelocity penetration theory.[6] It seems reasonable to assume that the quantity of light energy liberated at an impact site is related to the temperature achieved by the target and projectile. If this is the case, analysis of light flash data could be used to determine the state and temperature of matter during the crater formation process. It is likely that a larger fraction of microparticle kinetic energy is converted to light than is the case for more massive particles because of the short time required to form a crater. This implies that competing energy dissipation mechanisms which are time dependent have insufficient time to approach an equilibrium condition.

The first experiment conducted was designed simply to investigate the magnitude of the light flash as a function of particle parameters. This was accomplished by allowing particles from the accelerator to pass through a particle charge-velocity detector and to impact on a glass window whose surface was normal to the direction of the particle beam. An RCA 6199 multiplier phototube was optically coupled to the rear side of the window with Dow Corning 200 Fluid. The phototube was wired in a conventional manner with the photocathode at a negative 1000 volts and the anode at ground. The voltage divider used 240K resistors while a 100K anode resistor was used. The voltage signal at the anode was fed through a cathode follower amplifier to the "B" beam

of a Tektronix 555 oscilloscope. The particle detector signal was displayed on the "A" beam. The traces were photographed and analyzed in the usual manner.

It was felt that the results of the impact light flash should be similar to those obtained with the impact ionization effect. Consequently, the data were plotted in an identical manner as is illustrated in Fig. 8 where light flash peak amplitude, normalized to particle mass, is plotted as a function of velocity. It is immediately evident that the magnitude of the impact light flash increases extremely rapidly with velocity.

This may not be surprising when one considers the mechanism by which light is produced and the method by which it was measured. For purposes of discussion, let us assume that the source of light approximates a black body and emits the normal temperature dependent black body radiation. Near the threshold for light emission, which occurs at about 2 km/sec, it is likely that the temperature of the material near the impact site is a strong function of impact velocity. At much higher impact velocities this may not be the case because the temperature may be limited by other dissipative mechanisms. However, let us concern ourselves with the low velocity regime only. If the radiation detector were equally sensitive at all wavelengths, this velocity dependence could be observed directly, but this is not the case. The photomultiplier is sensitive over a fixed narrow wavelength region centered about 4400 $\mathring{A}$. Consequently, the radiant energy emitted in the spectral response region of the photomultiplier is not a constant fraction of the total radiant energy emitted for all temperatures because of the shape of the black body radiation curve. For example, a change in source temperature from 1000^{o}K to 2000^{o}K results in a change in radiant energy at 4400 $\mathring{A}$ of about seven orders of magnitude. The combination of velocity and temperature effects could easily lead to the observed velocity dependence.

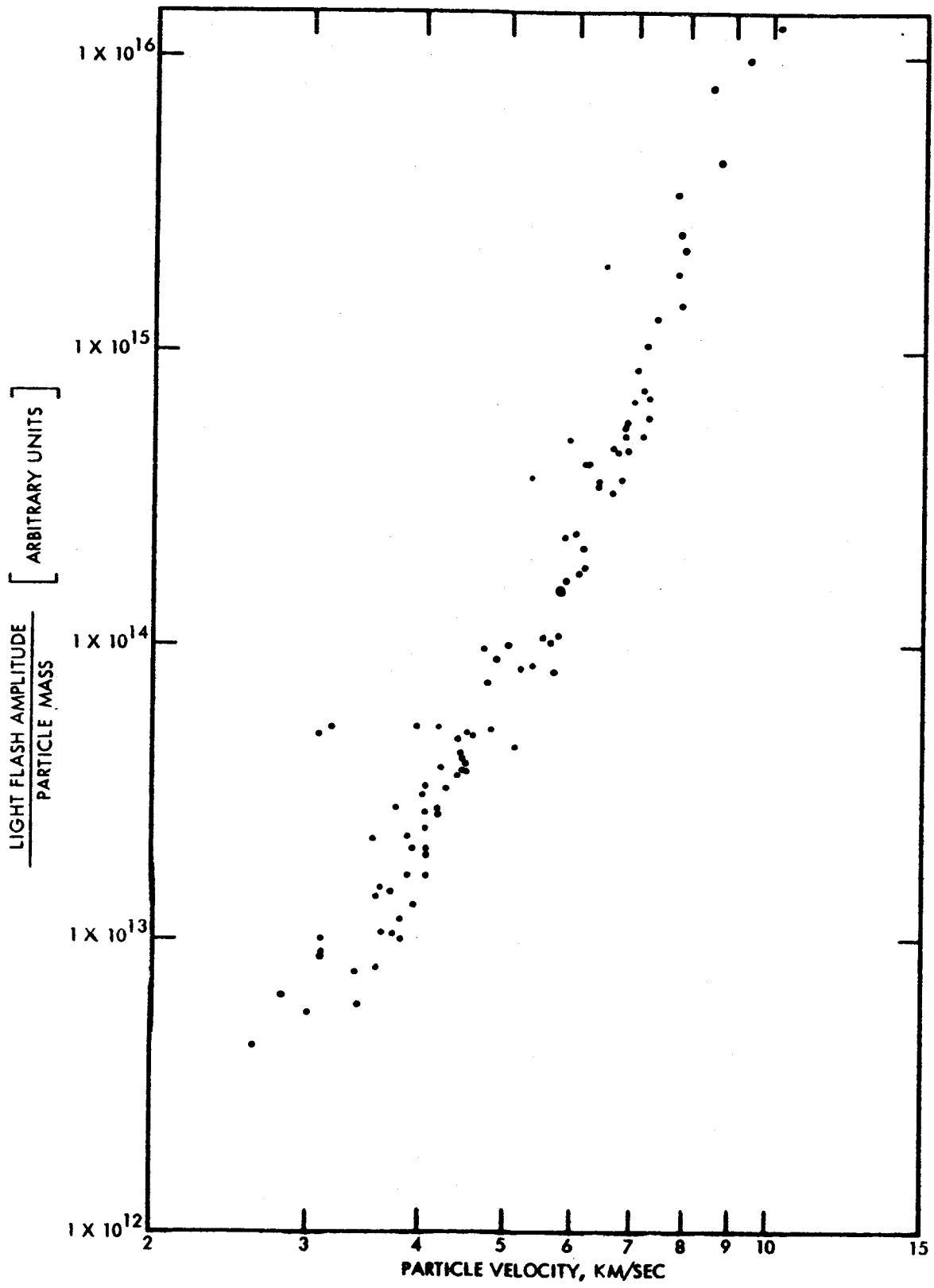

Figure 8. Light flash amplitude normalized to praticle mass as a function of particle velocity for a glass target.

The primary value of this particular experiment is that the results indicate the objectives of future experiments. For example, a number of the assumptions discussed above can be evaluated by using combinations of phototubes with different wavelength sensitivities. From this kind of experiment, one can estimate the temperature of the light producing source.

Some preliminary measurements were conducted on metallic targets as well. These measurements are confused by the emission of spray particles from the target which serve as secondary sources of light when they impact on surrounding surfaces. The existence of the secondary effect was verified by inserting a glass plate between the target and phototube at varying distances. The glass barrier reduces the time interval between the emission of radiation from the primary and secondary particles. In future experiments, the geometry of the light collection system will be designed to minimize the spray particle contribution.

C. Gaseous Target Impacts

Much of what is known about the natural meteoroid spectrum was deduced from the observation of visual meteors. There is little doubt that the mechanism by which a meteoroid entering the earth's atmosphere produces a luminous trail is generally understood. The incoming particle, traveling at a high velocity, collides with atmospheric molecules at high altitudes. Because of molecular bombardment at relatively high energies, the particle quickly heats up until its temperature becomes limited by vaporization or ablation. Vaporized atoms carry with them the meteoroid velocity. These atoms become excited by collisions with atmospheric gas molecules and emit visible radiation. Since the atmospheric density is low, the mean free paths are such that the evaporated atoms may radiate their excitation energy at large distances from the original meteoroid. A typical luminous trail is

10 or 20 kilometers long and several hundred meters in diameter. For most meteors the trail ends when the mass of the meteoroid has been vaporized.

There is widespread agreement on this general description, but the specific details of the various interactions involved are in doubt. Very little experimental data are available due, primarily, to the difficulty in performing experiments at hypervelocities and low gas pressures in the laboratory. For natural meteors, the aerodynamic flow is of the free molecular type, i.e., the mean free path of the gas molecules is much larger than particle dimensions. Thus, in order to simulate meteor phenomena with large high-speed particles, the gas pressure of the target must be very low and the interaction distances required for experiments would be hundreds of meters long. With small particles, however, the pressure of the gas may be adjusted so that the experiment can be performed within a few meters. The interpretation of experiments conducted with very small particles is aided by the fact that the particle is at substantially the same temperature throughout because of the short thermal time constant. In general, this is not the case for natural meteors. On the other hand, the drag forces acting on a natural meteor do not slow it down appreciably. For small particles the change in velocity because of drag forces must be taken into account.

In the usual formulation of meteor physics[7], the phenomenon of visual meteors is described by three equations, each containing an unknown constant. The first of these equations is the so-called drag equation which is given by

$$m \frac{dv}{dt} = -\Gamma \rho S v^2 \qquad (5)$$

where m is the mass, v the velocity, ρ the atmospheric density, S the cross-sectional area of the particle, and Γ is the drag coefficient. The value of the drag coefficient depends upon the geometry of the particle and the exact nature of the interactions of the gas molecules with the surface of the particle. A second meteor equation is the energy balance equation which describes the ablation of the meteor;

$$\zeta \frac{dm}{dt} = -\frac{\Lambda}{2} S\rho v^3 \quad , \tag{6}$$

where ζ is the heat of ablation or vaporation, and Λ is the fraction of incoming energy which heats the particle and is called the heat transfer coefficient. The third equation describes the intensity of light from a meteor trail and is given by

$$I = \frac{\tau}{2} \left(\frac{dm}{dt}\right) v^2 \quad , \tag{7}$$

where I is the light intensity and τ is the luminous efficiency.

In application of these equations to meteors, v, dv/dt, ρ, and I are measured by photographic techniques. Values of Γ, Λ, ζ, and τ are assumed. The value of m is obtained by the simultaneous solution of the three equations.

It can be recognized that the quantities Γ, Λ, and τ can be measured under certain conditions. In some respects the electrostatic accelerator is uniquely qualified for measurements of this kind. A fairly comprehensive investigation of this phenomenon has begun, and preliminary results have been described in an earlier report.[8] The experiments are accomplished by allowing particles from the accelerator to pass through a differential pumping system into a target chamber which is filled with gas at a few mm of Hg

pressure. The flight of the particle through the gas can be followed by two methods. When the particle first enters the gas, it retains its charge and its position can be monitored by means of charged particle detectors. At some point along its path, the particle absorbs sufficient energy to melt. At this time, the charge of the particle drops because a molten particle is unable to support a high electric field at its surface. Usually, however, sufficient charge remains to continue measurements with the charged particle detector. Still later, the particle reaches vaporization temperature and the charge on the particle is lost very rapidly. However, prior to this time, radiation is being emitted which can be observed with photomultiplier tubes. From the onset of light emission, the position of the particle is monitored by a linear array of photomultiplier tubes. This technique is applicable until the particle is completely vaporized or until it loses sufficient energy to stop radiating.

Our preliminary investigations have been concerned with measurements of the drag coefficient and the heat transfer coefficient under rather special conditions. The drag coefficient is determined by simply measuring the position as a function of time for a given particle and applying Eq. (5) above. We have measured the drag coefficient for gaseous targets of oxygen, argon, and air at pressures from one to two mm of Hg. In all cases the measured drag coefficient is nearly unity.

Values for the heat transfer coefficient were obtained for each of the target gases also. However, our measurements were made for the special case of a solid particle. For this special case, dm/dt is zero and Eq. (6) does not apply. To find λ (defined as the heat transfer coefficient for a solid particle) we equate the energy required to melt the particle to the energy delivered over the time required for the particle to reach its melting point, i.e.,

$$mC\,\Delta T = \int_0^{\tau} \frac{\lambda}{2}\,\rho A v^3\,dt \qquad (8)$$

where C is the specific heat and ΔT is the change in temperature. The integral was evaluated by direct measurement of v as a function of t for each particle. Assuming that the specific heat and the heat transfer coefficient are constants from room temperature to melting temperature, the values we obtained are as follow:

$$\lambda_{oxygen} = 1.06 \pm 0.03$$
$$\lambda_{argon} = 0.90 \pm 0.08$$
$$\lambda_{air} = 0.86 \pm 0.07 \quad .$$

It should be noticed that the value of λ for oxygen is greater than 1. This is not surprising since the iron of the particle and the oxygen can combine chemically to produce an apparent efficiency of greater than 100%.

Figure 9 illustrates the results of a typical experiment. It was from data like these that the values of λ and Γ were obtained. In Fig. 9, the velocity as a function of time was obtained by the charged particle type of detector. The temperature curve was computed using the experimental data and Eq. (8). The temperature curve has not been corrected for radiation losses, but the energy loss by radiation is very small compared to the rate of energy input to the particle. The light intensity as a function of time was obtained by the array of photomultiplier tubes mentioned above, but was not used for quantitative measurements. It is shown simply to demonstrate at what point appreciable radiation is observed.

In some respects the measurements described in the preceding paragraphs can be classified as molecular beam physics where the roles of the target and the gas have been reversed. These experiments are equivalent to bombarding a target with molecular beams with energies of from 1 to about 10 eV. This range of energies is

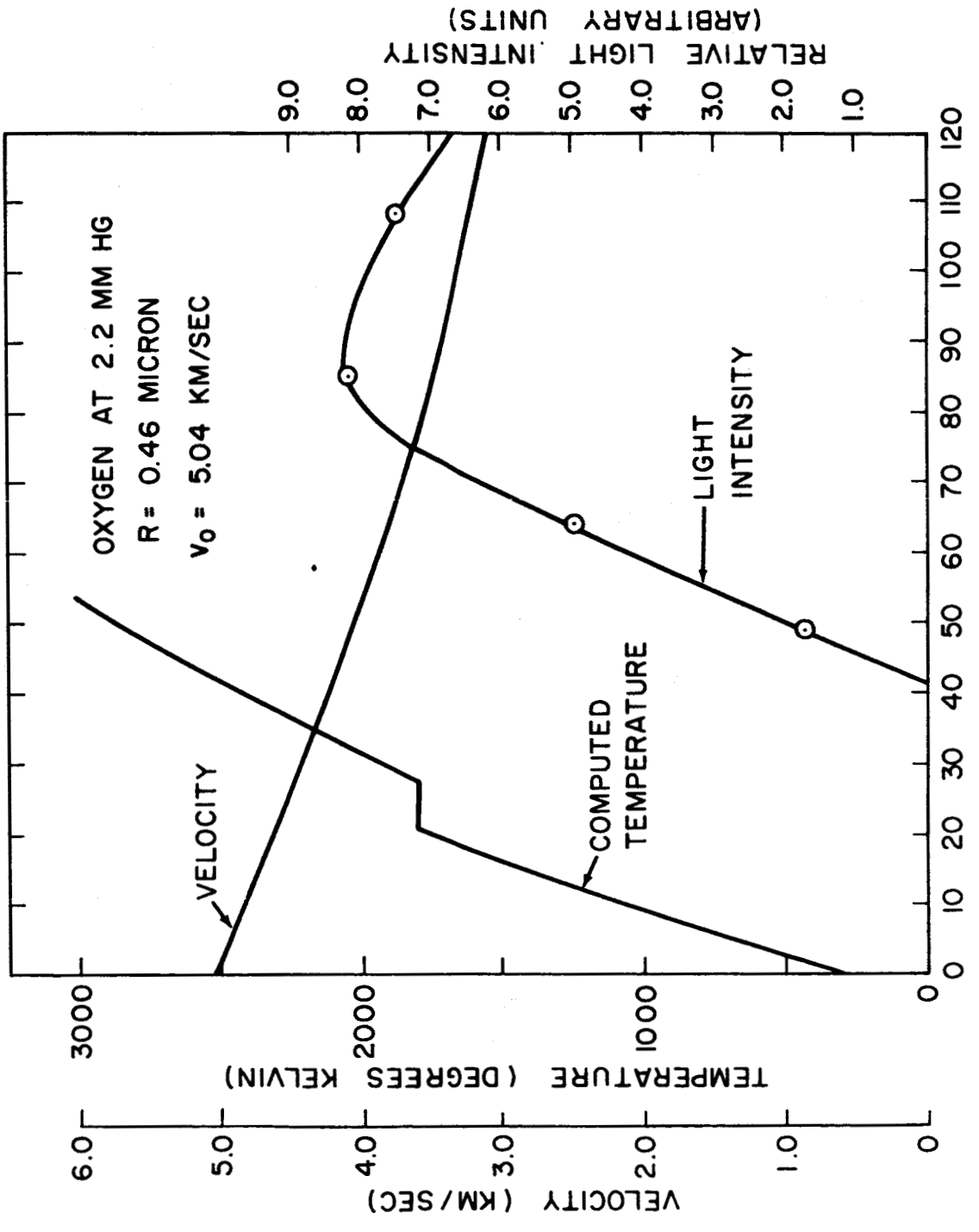

Figure 9. Curves illustrating the simulation of meteors.

extremely difficult to obtain by other techniques and we feel that a great amount of work remains to be done in this particular area.

D. Miscellaneous Tests and Experiments

In addition to the programs described above, STL facilities and personnel were utilized in tests of micrometeoroid detectors and sensor elements. The tests were usually done in conjunction with the NASA personnel who developed the instruments and quantitative data derived from the tests were retained by them.

The micrometeoroid detector scheduled for use on the EGO spacecraft is an example of an instrument subjected to a detailed test program. It is being developed by NASA scientists from Goddard Space Flight Center.

This detector is designed to measure direction, velocity, momentum, and possibly one other parameter of the impacting micrometeoroid. The detector consists of three separate units mounted in a mutually orthogonal array. Each unit, which is cylindrical in shape, is collimated so as to accept particles incident within a relatively small solid angle. The direction of the micrometeoroid is specified by noting which of the units is activated by the event and the orientation of the spacecraft.

The velocity is determined by a time-of-flight measurement. Signals to initiate and terminate the time-of-flight measurement are derived from two capacitor-type micrometeoroid detectors. The first of these is edge-supported in a plane perpendicular to the axis of the cylinder. The other one is affixed to the "sounding board" of an acoustical detector. The momentum of the micrometeoroid is derived from the acoustical detector signal. The first capacitor is extremely thin to minimize the energy loss suffered by the meteoroid in passing through it. The second capacitor detector is not so critical and may be composed of thicker elements if desired.

STL personnel have been involved with the EGO detector, since its inception. Originally, impact ionization detectors were proposed to generate the time-of-flight signals. However, tests indicated that the signals from a thin foil ionization detector were incompatible with the rest of the system. Consequently, the capacitor-type detector was evaluated. NASA personnel developed a capacitor which utilizes an aluminum oxide dielectric and vapor deposited aluminum conductor plates. The total thickness of a self-supporting capacitor of this type can be made as small as 1500 Å. The properties of a thin capacitor detector as a function of voltage were examined in a series of tests. At low applied voltages, say up to about 5 volts, no signals were observed. In the range from 5 to 20 volts the signal amplitude was proportional to particle parameters in much the same way as the impact ionization effect. At slightly higher voltages, say 30 volts or so, each particle initiated a complete voltage breakdown which healed itself. At still higher voltages spontaneous breakdown occurred. It was proposed to operate the detectors in the "proportional" region, thus providing a redundant measurement of mass and velocity.

Each component of a prototype unit was tested during the latest experiments with complete success.

IV. SUMMARY

Techniques developed under earlier contracts have been applied to experiments of a more definitive nature with encouraging results. More quantitative information on the impact light flash and impact ionization effects was obtained. The preliminary experiments on the interaction of high-speed particles with gaseous targets demonstrated the applicability of the electrostatic accelerator to meteor simulation. The EGO micrometeoroid detector was subjected to a comprehensive test program throughout its development which should be very useful in the interpretation of results obtained with it.

In summary, the versatility of the STL electrostatic accelerator has been amply demonstrated by the variety of meaningful experiments which have been conducted with it. Future experiments will be concerned with more refined measurements of some of the phenomena described above.

REFERENCES

1. H. Shelton, C. D. Hendricks, Jr. and R. F. Wuerker, J. Appl. Phys., Vol. 31, 1234, (1960).

2. J. F. Friichtenicht, Rev. of Sci. Inst., Vol. 33, 209 (1962).

3. J. F. Friichtenicht and J. C. Slattery, "Ionization Associated with Hypervelocity Impact", NASA Technical Note, NASA TN D-2091, August 1963.

4. Otto E. Berg and L. H. Meridith, Journal of Geophysical Research, Vol. 61, 751 (1956).

5. W. M. Alexander and O. E. Berg, the Fifth Symposium on Hypervelocity Impact, Denver, Colorado, November 1961.

6. R. L. Bjork, Proceedings of the Sixth Symposium on Hypervelocity Impact, Vol. II, August 1963.

7. F. L. Whipple and G. S. Hawkins, "Meteors", Handbuch der Physik, Vol. LII, Springer-Verlag, Berlin, 1959.

8. J. C. Slattery, J. F. Friichtenicht and B. Hamermesh, "The Interaction of Micrometeorites with Gaseous Targets", submitted for publication as a NASA Technical Note under NASA Contract NASw-561, STL Report 8699-6004-RU-000, July, 1963.

ro